SCIENCE CHINA
Technological Sciences

• Article •

October 2014 Vol.57 No.10: 2012–2019
doi: 10.1007/s11431-014-5654-6

Generatrix shape optimization of stiffened shells for low imperfection sensitivity

WANG Bo[1], HAO Peng[1*], LI Gang[1], WANG XiaoJun[2], TANG XiaoHan[2] & LUAN Yu[2]

[1] *State Key Laboratory of Structural Analysis for Industrial Equipment, Department of Engineering Mechanics, Dalian University of Technology, Dalian 116023, China;*
[2] *Beijing Institute of Astronautical Systems Engineering, Beijing 100076, China*

Received March 3, 2014; accepted May 10, 2014

According to previous studies, stiffened shells with convex hyperbolic generatrix shape are less sensitive to imperfections. In this study, the effects of generatrix shape on the performances of elastic and plastic buckling in stiffened shells are investigated. Then, a more general description of generatrix shape is proposed, which can simply be expressed as a convex B-spline curve (controlled by four key points). An optimization framework of stiffened shells with a convex B-spline generatrix is established, with optimization objective being measured in terms of nominal collapse load, which can be expressed as a weighted sum of geometrically imperfect shells. The effectiveness of the proposed framework is demonstrated by a detailed comparison of the optimum designs for the B-spline and hyperbolic generatrix shapes. The decrease of imperfection sensitivity allows for a significant weight saving, which is particularly important in the development of future heavy-lift launch vehicles.

stiffened shell, collapse, imperfection sensitivity, generatrix shape, optimization

Citation: Wang B, Hao P, Li G, et al. Generatrix shape optimization of stiffened shells for low imperfection sensitivity. Sci China Tech Sci, 2014, 57: 2012–2019, doi: 10.1007/s11431-014-5654-6

1 Introduction

Axially compressed thin-walled cylinders are very sensitive to various forms of imperfections. The extent of imperfection sensitivity is strongly related to R/t (ratio of shell radius to equivalent wall thickness), stiffened patterns, stacking sequence, etc. Based on a large collection of experimental data, knockdown factors (KDFs) of thin-walled cylinders with varying R/t were proposed in the most famous design guideline NASA SP-8007 [1]. However, these recommended values of KDF were proven to be overly conservative in recent studies [2–4], which may result in a weight redundancy for structural designs. Alternatively, more detailed modeling of structures and nonlinear analysis have been implemented in numerical methods, which are exactly suitable for predicting the knockdown effect on load-carrying capacity, since the load redistribution owing to the prebuckling bending caused by imperfections can be simulated accurately [5].

According to the Chinese National Medium- and Long-term Science Development Plans, the construction of space stations will be completed by about 2020, and several deep-space probes will be performed as the exploration of the moon proceeds. For this reason, the advance research of heavy-lift launch vehicles has been under way. As a major component of heavy-lift launch vehicles, fuel tanks are usually composed of stiffened shells, bulkheads and Y-rings, as shown in Figure 1. With the advent of heavy-lift launch vehicles, the value of R/t increases significantly compared with that known for current launch vehicles. This leads to extremely high imperfection sensitivity.

*Corresponding author (email: haopeng@dlut.edu.cn)

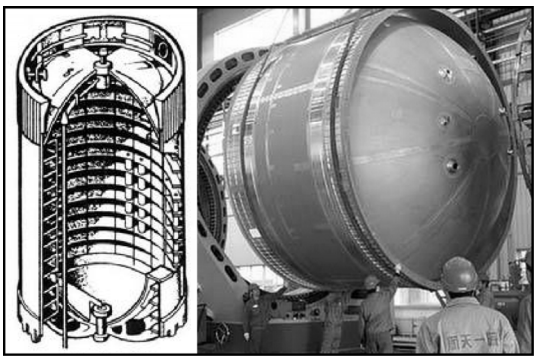

Figure 1 Schematic and photograph of the fuel tank in a typical launch vehicle.

Clearly, finding a robust design to resist and tolerate various forms of imperfections is of great significance for realistic stiffened shells, which is reflected in two aspects. One is increasing the load-carrying capacity of geometrically perfect stiffened shells, and the other is decreasing the imperfection sensitivity of these structures. Substantial studies have focused on the performance improvement or weight reduction of geometrically perfect stiffened shells [6−10]. Specifically, Leriche and Haftka [6] demonstrated the efficiency of the genetic algorithm in dealing with global optimization and discrete design variables for composite stiffened panels. An adaptive surroagate-based optimization procedure was proposed for the optimum design of stiffened shells subject to post-buckling by Wu et al. [9]. Furthermore, Hao et al. [11] developed a bi-step surrogate-based optimization framework with adaptive sampling for non-uniform stiffened shells. However, it should be emphasized that a remarkable increase in load-carrying capacity may be accompanied by a significant increase in imperfection sensitivity [12]. Yet as far as we are aware, there are only limited works on the subject of the reduction of imperfection sensitivity. An optimization procedure for thin-walled structures was formulated by Reitinger and Ramm [13], which included buckling behavior and imperfection sensitivity. Motivated by research in the field of biology [14], Wang et al. [15] proposed a concept of hierarchical stiffened shells to restrict the developments of out-of-plane deformations caused by imperfections. Hrinda [16] found that a cylindrical shell with a concave hyperbolic imperfection has a larger buckling load than that for the perfect cylinder, and stiffened shells with a convex hyperbolic generatrix shape were proven to be less sensitive to eigenmode-shape imperfections by Hao et al. [17]. Moreover, the load-carrying capacities and imperfection sensitivities of cylindrical shells with different geometries were compared in detail by Tomás and Tovar [18].

In this study, the effects of generatrix shape on the performances of elastic and plastic buckling stiffened shells are investigated. Then, a more general description of the generatrix shape is proposed, which can simply be expressed as a convex B-spline curve (controlled by four key points). From the viewpoint of manufacturing, the B-spline generatrix shape can be generated by current plastic processing technologies [19,20], which are tending to play an increasingly important role in the development of advanced manufacturing technologies. Later in this paper, an optimization framework of stiffened shells with a convex B-spline generatrix is established, with optimization objective being defined in terms of nominal collapse load, which can be expressed as a weighted sum of geometrically imperfect shells. From the viewpoint of reliability, the effectiveness of the proposed framework is demonstrated by the detailed comparison of the B-spline shape with hyperbolic generatrix shape optimum designs. Finally, the combination of internal pressure and axial compression is also considered for the purpose of verification.

2 Methodology

2.1 Linear buckling analysis

Various model details can be taken into account in a finite element analysis (FEA), such as cutouts, local enhancements, rounding chamfers, weld lines, etc.

A linear buckling problem can be stated as:

$$\left(\boldsymbol{K}_0 + P_{cr}^j \boldsymbol{G}\right)\boldsymbol{\varphi}_j = \boldsymbol{0}, \quad j = 1, 2, \cdots, n, \tag{1}$$

where $\boldsymbol{K}_0$ and $\boldsymbol{G}$ are the stiffness and stress stiffness matrices, respectively. $\boldsymbol{\varphi}_j$ is the jth eigenvector, P_{cr}^j is the jth eigenvalue, and the lowest eigenvalue is the critical buckling load.

But, since displacements at the critical buckling configuration are assumed to be small in linear buckling analysis, such analysis turns out to be inaccurate for the structures under consideration, because those structures show significantly nonlinear pre-buckling behavior.

2.2 Explicit dynamic analysis

Nonlinear explicit dynamic analysis allows investigation of the evolution of the deformed shape of stiffened panels, from pre-buckling to post-buckling [21,22].

For an explicit dynamic analysis, the equation of motion can be expressed as

$$\boldsymbol{M}\boldsymbol{a}_t = \boldsymbol{F}_t^{\text{ext}} - \boldsymbol{F}_t^{\text{int}} - \boldsymbol{C}\boldsymbol{V}_t - \boldsymbol{K}\boldsymbol{U}_t, \tag{2}$$

where $\boldsymbol{M}$ is the mass matrix, $\boldsymbol{C}$ is the damping matrix, $\boldsymbol{K}$ is the stiffness matrix, $\boldsymbol{a}$ is the vector of nodal acceleration, $\boldsymbol{V}$ is the vector of nodal velocity, $\boldsymbol{U}$ is the vector of nodal displacement, t is the time, $\boldsymbol{F}_t^{\text{ext}}$ is the vector of applied external force, and $\boldsymbol{F}_t^{\text{int}}$ is the vector of internal force.

It is possible to use explicit time integration with the

central difference method to approximate velocity and acceleration, as follow:

$$\boldsymbol{a}_t = \left(\boldsymbol{U}_{t-\Delta t} - 2\boldsymbol{U}_t + \boldsymbol{U}_{t-\Delta t}\right) / \Delta t^2, \tag{3}$$

$$\boldsymbol{V}_t = \left(\boldsymbol{U}_{t-\Delta t} - \boldsymbol{U}_{t-\Delta t}\right) / 2\Delta t, \tag{4}$$

where Δt is the time increment. Substituting eqs. (3) and (4) into eq. (2), the equation of motion is transformed into

$$\left(\frac{\boldsymbol{M}}{\Delta t^2} + \frac{\boldsymbol{C}}{2\Delta t}\right)\boldsymbol{U}_{t+\Delta t} = \boldsymbol{F}_t^{\text{ext}} - \boldsymbol{F}_t^{\text{int}} + \left(\frac{2\boldsymbol{M}}{\Delta t^2} - \boldsymbol{K}\right)\boldsymbol{U}_t - \left(\frac{\boldsymbol{M}}{\Delta t^2} - \frac{\boldsymbol{C}}{2\Delta t}\right)\boldsymbol{U}_{t-\Delta t}. \tag{5}$$

Referring to eq. (5), it can be seen that $\boldsymbol{U}_{t+\Delta t}$ depends on $\boldsymbol{U}_t$ and $\boldsymbol{U}_{t+\Delta t}$. The equations can be solved directly, and no convergence checks are required since the equations are uncoupled.

In general, it has been recognized that initial geometrical imperfections are a major contributor to the discrepancy between the predicted collapse loads and experimentally measured loads. In practice, imperfections of various forms are unavoidable for realistic structures, and imperfection sensitivities are highly related to *R*/*t*, stiffened pattern, and even stacking sequence, as well as other factors. Thus, the knockdown effects caused by imperfections should be considered in the design process. The geometry of an imperfect structure can be obtained by modifying the nodal coordinates according to the imperfection vector, which can be formulated as the deviations from the perfect geometry [23].

2.3 Surrogate-based optimization technology

The surrogate model is a mathematical model that approximates the multivariate input/output behavior of complex systems, built via the design of experiment and approximation method.

The radial basis function (RBF) model uses a linear combination of several basis functions expressed in terms of the Euclidean distance between sample data points [24]. The RBF model can be expressed as

$$R(\boldsymbol{x}) = \sum_{j=1}^{n} \lambda_j \varphi(r), \tag{6}$$

$$r = \left\| \boldsymbol{x} - \boldsymbol{x}_j \right\|, \tag{7}$$

where ϕ is the basis function, λ_j is the weight coefficient evaluated by fitting the model to the training data, $\boldsymbol{x}$ is the vector of design variables, $\boldsymbol{x}_j$ is the vector of design variables at the *j*th sampling point, *r* is the Euclidean distance between two sample data points, and *n* is the number of sampling points.

The RBF model was proven to be the most dependable method in most situations for global optimization in terms of accuracy and robustness, compared with the kriging and polynomial regression models [25].

To release the computational burden caused by the large number of iterations, surrogate models have been successfully utilized in the optimization of stiffened panels [26–28].

3 Effects of generatrix shape on the performance of elastic and plastic buckling in stiffened shells

3.1 Load-carrying capacity of perfect geometry

Two orthogrid stiffened shells (named S1 and S2) were established in this study, whose dimensions were identical to those in Hao et al. [17], and which are shown in Table 1 and Figure 2. Typical material elastic properties applied for the aluminum alloy being used in the model are: Young's modulus E=70 GPa, Poisson's ratio υ=0.33, and density ρ=2.7×10^{-6} kg/mm^3. Only the plastic properties of the two shells were different: For S1 and S2, respectively, yield stress σ_s=410 and 300 MPa, ultimate stress σ_b=480 and 400 MPa, and elongation γ=0.07 and 0.05. The finite element models of stiffened shells were established in ABAQUS software, as shown in Figure 2.

The boundary and load conditions were also the same as

Table 1 Values of the geometrical parameters for stiffened shells S1 and S2.

Item	Value
Diameter D (mm)	3000.0
Length L (mm)	2000.0
Skin thickness t_s (mm)	4.0
Stiffener thickness t_r (mm)	9.0
Stiffener height h (mm)	15.0
Number of circumferential stiffeners N_c	26
Number of axial stiffeners N_a	90

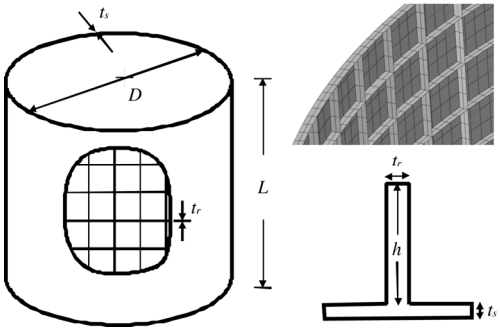

Figure 2 Schematic of each orthogrid stiffened shells S1 and S2.

those in Hao et al. [17]. Since the structural parameters and material elastic properties of S1 and S2 were identical, the linear buckling loads of the two shells were equal. However, owing to the influence of yield in the process of post-buckling analysis, the discrepancy of collapse patterns of the two shells is remarkable, as shown in Figure 3.

The effects of generatrix shapes on the load-carrying capacities of the two shells were then investigated. A hyperbolic generatrix shape was used first, as its description is concise. The range of the amplitude w/R (w being the amplitude of the hyperbolic vertex) was specified as [–0.05, 0.05], which was considered to be sufficiently small compared with the diameter. The collapse loads of the two shells with varying amplitudes of hyperbolic generatrix shape are shown in Figure 4. As can be seen, the trend of the curve for S1 is different from that of S2. With the increase of w/R, the collapse load of S1 increases at first and then decreases slightly. This effect may be because of the difference between the collapse deformation shapes of the two shells, as is evident in Figure 3. In the case of elastic buckling, the collapse mainly occurs at the mid-bay of the shell and is referred to as the "diamond shaped" mode. Conversely, in plastic buckling, the collapse usually evolves from both ends of the shell, referred to as the "elephant foot" mode [29]. The variation of generatrix shape results in a stiffness redistribution along the shell length, and the difference in collapse deformation shapes between the elastic and plastic buckling of the shells leads to the discrepancy in the two curves shown in Figure 4.

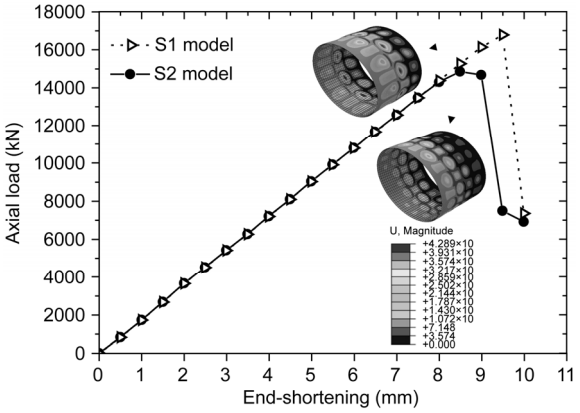

Figure 3 Load versus end-shortening curves of S1 and S2, together with the deformed shapes at collapse loads.

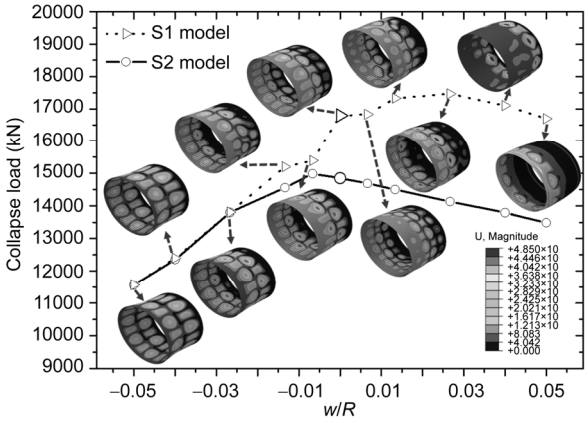

Figure 4 Effects of hyperbolic generatrix shapes on the load-carrying capacities of S1 and S2 models.

3.2 Load-carrying capacity of imperfect geometry

In this subsection, imperfection sensitivity is taken into account. According to previous studies, eigenmode-shape imperfection is commonly adopted at the preliminary design stage of thin-walled structures [30]. The European standard for steel shell structures [31] recommends that the imperfection should be specified in the form of eigenmode shape, with its amplitude linked to fabrication quality, unless a different unfavourable pattern is justified. For this reason, eigenmode-shape imperfections were utilized in the assessment of load-carrying capacities in this study. Two typical amplitudes δ were selected to represent the small-and large-amplitude imperfections, with δ=1.9 mm (α=0.1) and δ=19.0 mm (α=1.0) corresponding to a one-tenth and unity, respectively, sum of skin thickness and stiffener height, where α is the non-dimensional imperfection amplitude, defined by $\alpha = \delta / \left(h + t_s\right)$.

The collapse loads of the two shells S1 and S2 with varying amplitudes of hyperbolic generatrix shape are shown in Figure 5, where $P_{0.1}$ stands for the collapse load of stiffened shells with small-amplitude imperfections, and $P_{1.0}$ is the collapse load of stiffened shells with large-amplitude imperfections. Unlike the load-carrying capacity of perfect geometry, it can be found that the collapse loads of the two shells with imperfections demonstrate monotonically increasing trends with an increase of w/R, either for $P_{0.1}$ or for $P_{1.0}$. This may be attributed to the reason that, once the imperfection is introduced into the perfect model, the collapse

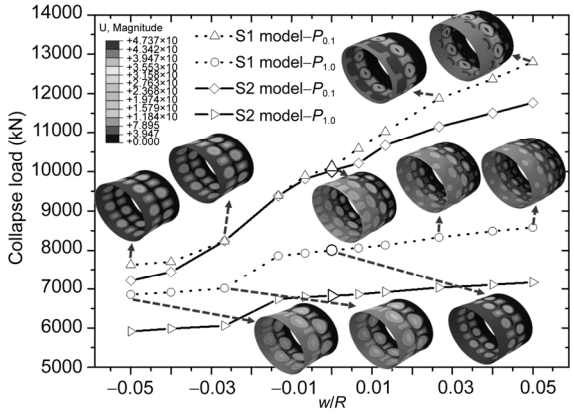

Figure 5 Effects of hyperbolic generatrix shapes on the load-carrying capacities of S1 and S2 models with small- and large-amplitude eigenmode-shape imperfections.

of the model would occur before material yielding is reached, and so the effect of generatrix shape on the collapse load, in this case, is typically similar to the one for the elastic buckling model, i.e. the S1 model without imperfections. Consequently, detailed study of elastic buckling in a shell is more meaningful, as imperfections are unavoidable in practice. The convex generatrix shape is a good choice to resist imperfections; however, the exact shape parameters need to be investigated in detail.

4 Generatrix optimization framework for low imperfection sensitivity

4.1 Formulation of generatrix shape

In this study, a more general description of generatrix shape has been developed, which can be controlled by four key points according to the symmetry with respect to the middle length section, as shown in Figure 6. Specifically, four control points are distributed uniformly along the shell length, and the B-spline passes through these four points. The B-spline can maintain the smoothness of the shell surface and thus reduce the risk of fuel leak. Also, as a result of its simplicity and flexibility, the B-spline shape has been applied to the design of curvilinear stiffeners [32].

Because it has been demonstrated that a convex generatrix shape can reduce imperfection sensitivity for stiffened shells, the radial deviations of the control points from the cylindrical shell, r_1, r_2 and r_3, are imposed to be positive, and the range of r_i/R is [0.0, 0.05]. Owing to the requirements of assembly at both ends of the shell, the control point P_0 is assumed to be fixed.

4.2 Generatrix shape optimization for low imperfection sensitivity

According to Reitinger and Ramm [13], the conventional optimum design is usually accompanied by a large degree of imperfection sensitivity, as optimizations often result in economic, lightweight and thin-walled structures. From a comparison of Figures 4 and 5, it is also evident that the optimum values of w/R are different for perfect and imperfect geometries. This enhances the significance of taking the influence of imperfections and the resulting decrease of the load-carrying capacity into the design criteria.

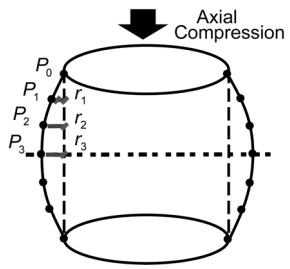

Figure 6 Schematic of the generatrix shape controlled by the B-spline.

As explained in section 3.2, once the imperfection is considered, the collapse of the model would occur before material yielding is reached, which is referred to as elastic buckling. Thus, only the S1 model needs to be discussed below. Eigenmode shape is also selected as the illustrative imperfection herein. Nominal collapse load is defined in order to evaluate both the load-carrying capacity of a geometrically perfect stiffened shell and its imperfection sensitivity, which can be expressed as a weighted sum of collapse loads of stiffened shells with small- and large-amplitude imperfections. The relevant variables include r_1, r_2 and r_3. The formulation of this optimization problem can be stated as

Maximize:

$$P_{\text{nom}} = \beta_1 P_{0.1} + \beta_2 P_{1.0}, \tag{8}$$

subject to

$$\beta_1 + \beta_2 = 1, \tag{9}$$

and

$$0.0 \leqslant r_i / R \leqslant 0.05, \ i = 1, \ 2, \ 3, \tag{10}$$

where β_1 and β_2 are the weighted coefficients of two collapse loads, which are set as 0.5 for simplicity herein.

The CPU time of a post-buckling analysis of the illustrative stiffened shell is about 1.8 h, using a PC with an Intel^{R} Core^{TM} i5 CPU with 2.9 GHz and 4 GB of RAM. A surrogate model is employed in this study in order to release the computational burden caused by the large number of iterations during optimization. Typically, a surrogate-based optimization is composed of inner optimizations and outer updates. Actually, the inner optimization is entirely based on the surrogate model and thus needs negligible computational capacity. The optimization is considered to be converged if the relative error between the results predicted by the surrogate model and that obtained by a FEA is less than 0.1%; otherwise, the surrogate model is refitted by both previous and new sampling data, and another inner optimization is carried out based on the newly built surrogate model.

According to the proposed values of sample numbers [25], a set of 125 sampling points is generated using the optimal latin hypercube sampling (OLHS), and a RBF model is then built based on the sampling data. To evaluate the quality of this RBF model, another sample set composed of 18 sampling points is generated by OLHS. Three metrics [11] including, $\%RMSE$, $\%AvgErr$ and $\%MaxErr$, are calculated by this sample set, which are 4.0%, 2.8% and 8.7% for $P_{0.1}$, and 4.3%, 3.5% and 9.4% for $P_{1.0}$, indicating an acceptable accuracy. Subsequently, a multi-island genetic algorithm (MIGA) is adopted in the surrogate-based optimization to find the optimum design, which has been pop-

ular in this field because of its intuitiveness, ease of implementation, and the ability to effectively solve highly nonlinear problems [33]. In MIGA, the population in one generation is divided into several islands, and the genetic operations are performed independently on each island. This independence enables the calculation to avoid converging local optimums [34].

For the purpose of concision, iterations based on the surrogate model have been removed, and only the history of outer updates has been preserved, as shown in Figure 7. After the evolution of five outer updates, the optimum design is achieved with r_1/R=0.0071, r_2/R=0.0473 and r_3/R=0.0399, respectively. The critical buckling load of the optimum design is 14679 kN, with the eigenmode shown in Figure 8. The collapse load obtained by a nonlinear explicit dynamic analysis is 15628 kN, and the predicted deformed shape at the collapse load is shown in Figure 9.

4.3 Comparison of different designs

For the purpose of comparison, the performances of the initial design and two optimum designs are listed in Table 2, including the critical buckling loads of three perfect shells as well as the collapse loads of three perfect and imperfect shells. For the hyperbolic shape optimum design (w/R=0.05, as is evident in Figure 5), the critical buckling load of the perfect shell is improved in a large amplitude compared with the initial design, while the increases of $P_{1.0}$ and P_{nom} are not so significant, and the collapse load of the perfect shell is even decreased. The B-spline shape optimum design gains a large increase in $P_{1.0}$ and thus P_{nom} compared with the initial design and the hyperbolic shape optimum design, representing a case of higher reliability.

Moreover, eigenmode-shape imperfection sensitivity curves can be compared for the initial design and two optimum designs, as shown in Figure 10. Initially, the collapse load of the B-spline shape optimum design is lower than that for the hyperbolic shape optimum design and the initial design. For the sufficiently small-amplitude imperfections, i.e. $0<\alpha<0.15$, the B-spline shape optimum design has higher load-carrying capacities than the initial design, but lower capacities than the hyperbolic shape optimum design. For for the medium- and large-amplitude imperfections, i.e. $0.15<\alpha<1.0$, a remarkable improvement of load-carrying capacity is found for the B-spline shape optimum design, compared with the other two designs. Generally, the imperfection sensitivity curve for each of the three designs can be divided into two phases: One steep descent phase and one relatively stable phase. The steep descent phase of the B-spline shape optimum design is seen to be shorter than

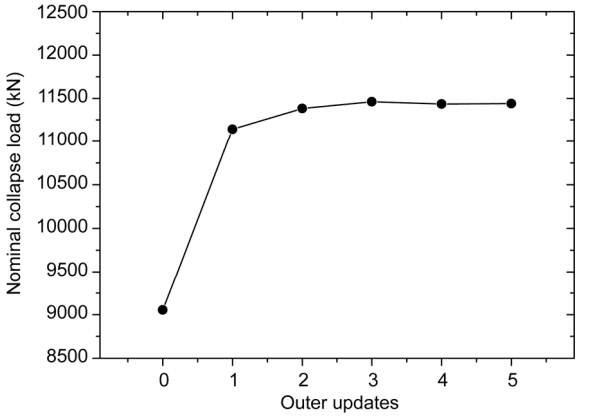

Figure 7 History of the outer updates in the surrogate-based optimization.

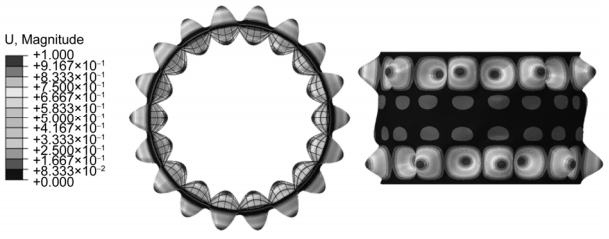

Figure 8 Eigenmode shape of the B-spline shape optimum design.

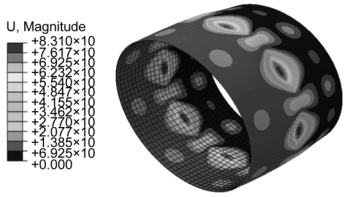

Figure 9 Deformed shapes of the B-spline shape optimum design at the collapse load.

Table 2 Comparison of the performances of different designs

Item	Initial design (S1 model)	Hyperbolic shape optimum design	B-spline shape optimum design
P_{cr} (kN)	13610	17737	14679
P_{co} (kN)	16792	16695	15628
$P_{0.1}$ (kN)	10106	12806	12121
$P_{1.0}$ (kN)	8003	8578	10759
P_{nom} (kN)	9055	10692	11440

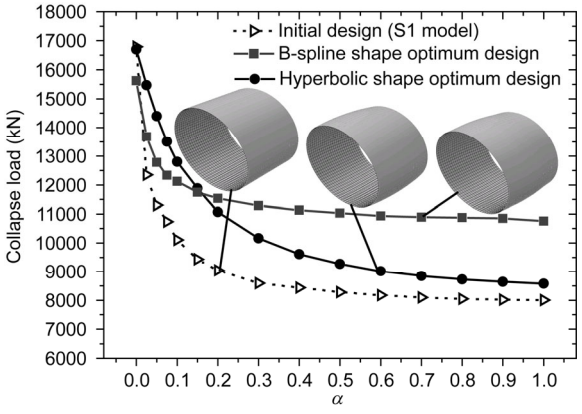

Figure 10 Eigenmode-shape imperfection sensitivity curves for the initial design and two optimum designs.

the other two designs. For both phases, the curve of the B-spline shape optimum design is more stable and finally converges to a higher value, which means that the variation in imperfection amplitude has little influence on the performance fluctuation of the design.

From a practical point of view, the convex generatrix shape is universal for pressure vessels, which can be caused by the internal pressure and relatively high stiffness at both ends. For the purpose of verification, the combination of internal pressure and axial compression is also considered for two optimum designs. Specifically, the internal pressure is 0.15 MPa, and the total loading time takes a value of 300 ms, which is composed of a pressure loading process and an axial compression loading process. From 0 to 100 ms, there is an increase in the internal pressure linearly from zero to the maximum value 0.15 MPa; then from 100 to 300 ms, keeping the internal pressure as a constant status, the axial compression load increases proportionally from zero to the maximum until collapse occurs. The corresponding load versus end-shortening curves of two optimum designs with $\alpha = 1.0$ are shown in Figure 11. The collapse loads of the B-spline shape optimum design and the hyperbolic shape optimum design are 11308 and 9358 kN, respectively, which are even higher than those for stiffened shells under purely axial compression. Thus, it can be concluded that the condition of purely axial compression gives a safe estimation for practical designs of stiffened shells with various generatrix shapes.

The stiffened shell of B-spline shape can be fabricated by current plastic processing technologies, such as power spinning forming, spin forging and tube spinning [35]. With the rapid development of plastic processing technologies, the high quality, high efficiency, low consumption, and good flexibility of the manufacturing of stiffened shells with B-spline generatrix shapes could finally be achieved. This type of conceptual design is expected to be utilized in the future heavy-lift launch vehicles.

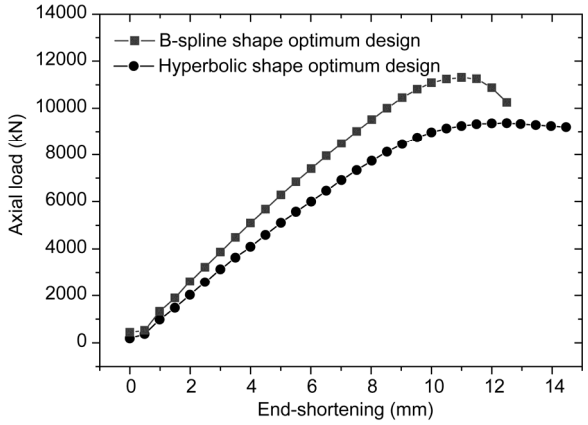

Figure 11 Load versus end-shortening curves for two optimum designs under internal pressure and axial compression.

5 Conclusions

In this paper, the effects of generatrix shape on the performances of elastic and plastic buckling in stiffened shells have been investigated. The generatrix shapes have been found to exert different influences on the collapse loads of the two types of perfect shells examined, while the collapse loads of both types of shells with imperfections show monotonically increasing trends with increasing amplitudes of convex hyperbolic generatrix shape.

A more general description of generatrix shape has been proposed, which can simply be expressed as a convex B-spline curve (controlled by four key points). An optimization framework of stiffened shells with a convex B-spline generatrix has been established, with optimization objective being defined in terms of nominal collapse load, which can be expressed as a weighted sum of geometrically imperfect shells. The effectiveness of the proposed framework has been demonstrated by a detailed comparison of the B-spline shape and hyperbolic generatrix shape optimum designs.

The decrease of imperfection sensitivity allows for a significant weight saving, which is particularly important in the development of future heavy-lift launch vehicles.

This work was supported by the National Basic Research Program of China ("973" Project) (Grant Nos. 2014CB049000, 2014CB046596), the National Natural Science Foundation of China (Grant Nos. 11402049, 11372062), the Project funded by China Postdoctoral Science Foundation (Grant No. 2014M551070), the Fundamental Research Funds for Central University of China (Grant No. DUT14RC(3)028), and the "111" Program (Grant No. B14013).

1 Weingarten V I, Seide P, Peterson J P. Buckling of thin-walled circular cylinders. NASA SP-8007, 1968
2 Arbocz J, Starnes J H. Future directions and challenges in shell stability analysis. Thin-Walled Struct, 2002, 40: 729–754
3 Hühne C, Rolfes R, Breitbach E, et al. Robust design of composite cylindrical shells under axial compression-simulation and validation. Thin-Walled Struct, 2008, 46: 947–962
4 Wang B, Hao P, Li G, et al. Determination of realistic worst imperfection for cylindrical shells using optimization algorithm. Struct Multidiscip Optim, 2013, 48: 777–794
5 Hilburger M W, Starnes J H. Effects of imperfections of the buckling response of composite shells. Thin-Walled Struct, 2004, 42: 369–397
6 Leriche R, Haftka R T. Optimization of laminate stacking sequence for buckling load maximization by genetic algorithm. AIAA J, 1993, 31: 951–956
7 Bushnell D, Bushnell W D. Minimum-weight design of a stiffened panel via PANDA2 and evaluation of the optimized panel via STAGS. Comput Struct, 1994, 50: 569–602
8 Venkataraman S, Lamberti L, Haftka R T. Challenges in comparing numerical solutions for optimum weights of stiffened shells. J Spacecraft Rockets, 2003, 40: 183–192
9 Wu H, Yan Y, Yan W, et al. Adaptive approximation-based optimization of composite advanced grid-stiffened cylinder. Chin J Aeronaut, 2010, 23: 423–429
10 Vescovini R, Bisagni C. Buckling analysis and optimization of stiffened composite flat and curved panels. AIAA J, 2012, 50: 904–915

11 Hao P, Wang B, Li G. Surrogate-based optimum design for stiffened shells with adaptive sampling. AIAA J, 2012, 50: 2389–2407
12 Obrecht H, Rosenthal B, Fuchs P, et al. Buckling, postbuckling and imperfection-sensitivity: Old questions and some new answers. Comp Mech, 2006, 37: 498–506
13 Reitinger R, Ramm E. Maximizing structural efficiency including buckling and imperfection sensitivity. In: Proceedings of 5th AIAA/USAF/NASA/ISSMO Symposium on Multidisciplinary Analysis and Optimization. Panama City Beach, 1994. 1228–1238
14 Gao H, Ji B, Jäger I L, et al. Materials become insensitive to flaws at nanoscale: Lessons from nature. Proc Natl Acad Sci USA, 2003, 100: 5597– 5600
15 Wang B, Hao P, Li G, et al. Optimum design of hierarchical stiffened shells for low imperfection sensitivity. Acta Mech Sin, 2014, 30: 391–402
16 Hrinda G A. Effects of shell-buckling knockdown factors in large cylindrical shells. In: Proceedings of 5th International Conference on High Performance Structures and Materials. Tallinn, Estonia, 2010
17 Hao P, Wang B, Li G, et al. Surrogate-based optimization of stiffened shells including load-carrying capacity and imperfection sensitivity. Thin-Walled Struct, 2013, 72: 164–174
18 Tomás A, Tovar J P. The influence of initial geometric imperfections on the buckling load of single and double curvature concrete shells. Comput Struct, 2012, 96: 34–45
19 Yang H, Zhan M, Liu Y L, et al. Some advanced plastic processing technologies and their numerical simulation. J Mat Process Technol, 2004, 151: 63–69
20 Li C, Yang H, Zhan M, et al. Effects of process parameters on numerical control bending process for large diameter thin-walled aluminum alloy tubes. Trans Nonferrous Met Soc China, 2009, 19: 668–673
21 Lanzi L. A numerical and experimental investigation on composite stiffened panels into post-buckling. Thin-walled Struct, 2004, 42: 1645–1664
22 Lanzi L, Giavotto V. Post-buckling optimization of composite stiffened panels: Computations and experiments. Compos Struct, 2006, 73: 208–220
23 Hao P, Wang B, Li G, et al. Worst Multiple Perturbation Load Approach of stiffened shells with and without cutouts for improved knockdown factors. Thin-Walled Struct, 2014, 82: 321–330
24 Dyn N, Levin D, Rippa S. Numerical procedures for surface fitting of scattered data by radial functions. SIAM J Sci Stat Comput, 1986, 7: 639–659
25 Jin R, Chen W, Simpson T W. Comparative studies of metamodelling techniques under multiple modelling criteria. Struct Multidiscip Optim, 2001 23: 1–13
26 Vitali R, Park O, Haftka R T, et al. Structural optimization of a hat-stiffened panel using response surfaces. J Aircraft, 2002, 39: 158–166
27 Rikards R, Abramovich H, Kalnins K, et al. Surrogate modeling in design optimization of stiffened composite shells. Compos Struct, 2006, 73: 244–251
28 Marín L, Trias D, Badalló P, et al. Optimization of composite stiffened panels under mechanical and hygrothermal loads using neural networks and genetic algorithms. Compos Struct, 2012, 94: 3321–3326
29 Mazzolani F M, Mandara A, Di Lauro G. Plastic buckling of axially loaded aluminium cylinders: A new design approach. In: Proceedings of 4th International Conference on Coupled Instabilities in Metal Structures. Rome, Italy, 2004
30 Teng J G, Song C Y. Numerical models for nonlinear analysis of elastic shells with eigenmode-affine imperfections. Int J Solids Struct, 2001, 38: 3263–3280
31 Anonymous. General rules-supplementary rules for the strength and stability of shell structures. Eurocode 3, 1999
32 Mulani S B, Slemp W C H, Kapania R K. EBF3PanelOpt: An optimization framework for curvilinear blade-stiffened panels. Thin-walled Struct, 2013, 63: 13–26
33 Panda S, Padhy N P. Comparison of particle swarm optimization and genetic algorithm for FACTS-based controller design. Appl Soft Comput, 2008, 8: 1418–1427
34 Reiko T. Distributed genetic algorithms. In: Proceedings of 3rd ICGA. San Francisco, 1989
35 Wong C C, Dean T A, Lin J. A review of spinning, shear forming and flow forming processes. Int J Mach Tools Manuf, 2003, 43: 1419–1435